Original Article

Comparative Histological Study on the Preventive Role of Acarbose and Calcipotriol/Betamethasone in Mouse Model of Psoriasis-Like Skin Inflammation Induced by Imiquimod

Sarah Mohammed Alghandour, Marwa Mohamed Sabry and Manal Ali Abdel Mohsen

Department of Histology, Faculty of Medicine, Cairo University, Egypt

ABSTRACT

Introduction: Psoriasis is an autoimmune skin disorder that is symptomized by erythema and scaling. Recently, imiquimod (IMQ) has been used to induce skin inflammation in mice to create a psoriasis model.

Aim of the Work: To assess the possible preventive potential of acarbose on psoriasis-like skin inflammation induced by IMQ in adult male mice, and to compare it to calcipotriol/betamethasone applied on the same psoriasis mouse model.

Materials and Methods: Thirty four BALB/c mice were classified as the following groups: I(Control), II(IMQ): IMQ-model with topically applied Aldara cream, III(Acarbose): IMQ-model treated with Glucobay orally, IV(Calcipotriol/Betamethasone): IMQ-model treated with Calcipoheal-Cort ointment and V(Acarbose+Calcipotriol/Betamethasone): IMQ-model treated with both Glucobay and Calcipoheal-Cort combined. Haematoxylin & Eosin stain and S100 immunohistochemical staining were performed along with electron microscopic study of skin sections. Mean epidermal thickness and mean number of S100 immuno-positive keratinocytes were measured and measurements were statistically analyzed.

Results: Group II mice showed psoriasis-like signs of skin inflammation. Groups III and IV mice showed less signs of inflammation which were markedly attenuated by combination of both of the treatments. Group II demonstrated significant acanthosis and abundant infiltrates of inflammatory cells in the dermis and significantly numerous S100 immuno-positive keratinocytes. Groups III and IV showed significant improvement of these changes which were markedly diminished in group V as it showed almost normal histological structure.

Conclusion: Acarbose had an overall beneficial effect on psoriasis-mimicking mouse model triggered by IMQ, almost comparable to that demonstrated by calcipotriol/betamethasone. However, combination of both treatments exerted a more powerful therapeutic effect.

Received: 09 July 2019, **Accepted:** 19 August 2019

Key Words: Acarbose; betamethasone; calcipotriol; imiquimod; psoriasis disease.

Corresponding Author: Sarah Mohammed Alghandour, MD, Department of Histology, Faculty of Medicine, Cairo University, Cairo, Egypt, **Tel.**: +20 1006208173, **E-mail:** sarah_alghandour@hotmail.com

ISSN: 1110-0559, Vol. 43, No. 1

INTRODUCTION

Psoriasis is a disfiguring autoimmune skin disorder, with reported prevalence ranging between 0.09% and 11.4% of the population worldwide, making it a significant global problem[1]. Psoriasis is a multifactorial disease as genetic factors have a role in enabling its development when they interact with environmental factors such as stress and certain medications[2, 3, and 4]. As an inflammatory disorder, patients suffering from psoriasis are at a great risk of developing metabolic disorders as insulin resistance and cardiovascular diseases[5]. Furthermore, the disfiguration resulting from psoriatic skin lesion causes severe psychological distress to psoriatic patients[6].

The main characters of psoriasis are uncontrolled proliferation of keratinocytes and their abnormal differentiation leading to development of focal erythematous scaly patches which shed constantly. Moreover, a cellular reaction that includes T lymphocytes, dendritic cells (DCs), macrophages and mast cells is involved in psoriasis pathogenesis[7,8].

Imiquimod (IMQ) is toll-like receptor (TLR) 7 agonist in mice and TLR 7 and 8 agonist in humans[6]. Imiquimod is prescribed to treat certain viral skin diseases as well as basal cell carcinomas[3]. However, it can also provoke a psoriasis-like disease in some patients as a side effect[9]. Similarly, topical application of IMQ to the skin of BALB/c mice induces lesions that mimics psoriasis being marked by keratinocytes hyperproliferation along with cellular inflammatory infiltration of DCs and T lymphocytes. Recently, IMQ-induced skin inflammation has been growingly used as mouse model to study human psoriasis[10,11].

 DOI: 10.21608/ejh.2019.13868.1132

Certain cells of the immune system and their inflammatory factors play the key role in psoriasis pathogenesis[12]. Researches have revealed that T helper 17 (Th17) cells and the inflammatory cytokines they produce especially interleukin (IL)-23 are detected in psoriatic lesions[10]. This IL-23/Th17 axis constitutes an essential element in the pathological process of psoriasis studied in humans as well as the IMQ mouse model[13].

To date, no therapy has been able to completely cure psoriasis. However, the past few years have witnessed remarkable advances in studying the pathogenesis of psoriasis, nonetheless, complete explanation of this disease is still far ahead[14]. Current treatment choices for psoriasis include steroids and vitamin D derivatives. Recently, it has been recognized that glucose metabolism plays a pivotal role in the mechanism of chronic inflammatory skin diseases. Accordingly, targeting metabolism is now considered as a promising method of managing psoriasis[15].

Acarbose, an alpha-glucosidase inhibitor, is a widely prescribed antidiabetic drug. It is considered to be a well-tolerated drug, besides, it doesn't cause hypoglycemia as long as other antidiabetic agents are not used concomitantly[16]. Through anti-inflammatory effects, acarbose decreases the inflammatory markers detected in diabetic patients[17]. Additionally, it also lowers the risk of diabetes mellitus (DM) major complications as cardiovascular diseases, which are marked by the presence of high levels of inflammatory factors[18].

S100 proteins are a family of multifunctional small proteins involved in proliferation, differentiation and intercellular adhesion[19]. Under normal states, production of inflammatory factors such as antimicrobial peptides (AMPs) is limited to possible points of microbial entrance in the epidermis, such as around the hair follicles[20]. Nevertheless, S100 proteins are over expressed in psoriatic skin, which is attributed to altered epidermal differentiation, and this happens because of the location of S100 encoding genes within the epidermal differentiation complex that contains major genes involved in epidermal differentiation[21].

The present work was structured to assess the possible preventive potential of acarbose on psoriasis-like lesion induced by IMQ in the skin of adult male BALB/c mice, and to compare it to the combined therapeutic effect of the widely used psoriasis medications, vitamin D analogue "calcipotriol" and corticosteroid "betamethasone", applied on the same psoriasis mouse model.

MATERIALS AND METHODS

I- Animals

Thirty four adult male BALB/c mice with average body weight 40 g, were housed in the animal house of Kasr Al-Ainy, Faculty of Medicine, Cairo University. The mice were treated according to the guidelines for animal research approved by Animal Ethics Committee, Faculty of Medicine, Cairo University. They were sub-caged in a conventional clean facility at 22–26◦C and allowed food and water ad libitum.

II- Materials

- Imiquimod (IMQ) (Aldara 5% cream, supplied in the form of sachets each containing 250 mg of cream, 3M Health Care Limited, Loughborough, Leicestershire, United Kingdom).
- Acarbose (Glucobay 50, supplied in the form of tablets each containing 50 mg acarbose, Bayer Pharma AG Leverkusen, Germany). The tablets were crushed and the required dose was weighed using a digital scale and dissolved in water.
- Calcipotriol and Betamethasone (Calcipoheal-Cort topical ointment containing calcipotriol 0.005% and betamethasone 0.05%, Advanced Pharmaceutical Industries Company (APIC), Cairo, Egypt).
- Anti-S100 antibody Rabbit polyclonal anti-S100 antibody, PA1-932, Thermo Fisher Scientific, Rockford, USA.

III- Experimental Design

The back skin of all mice was shaved 48 hours before the start of the study[22], then they were divided into 5 groups:

Group I (Control group n=10): Mice of this group were equally divided into two subgroups:

Subgroup Ia: Vaseline cream (Unilever, London, United Kingdom) was applied topically on the back skin of control group mice once daily for 6 successive days[23].

Subgroup Ib: Received 2 ml water orally by gastric gavage twice daily starting one week before induction of skin inflammation as detailed in group II, then continued till the end of the experiment[24].

Group II (IMQ group n=6): Aldara cream was applied topically on the back skin of IMQ group mice at a dose of 62.5 mg once daily for 6 successive days to induce psoriasis-like skin inflammation[25]. This equals a dose of 3.125 mg of the active compound daily which was proven to cause the most optimal inflammation of skin in mice[26].

Group III (Acarbose group n=6): Mice of this group received 500 mg/Kg Glucobay (=20 mg) dissolved in 2 ml water orally by gastric gavage twice daily starting one week before induction of skin inflammation as detailed in group II, then continued till the end of the experiment[24].

Group IV (Calcipotriol/Betamethasone group n=6): Skin inflammation was induced as detailed in group II. Calcipoheal-Cort ointment was simultaneously applied to the skin twice daily till the end of the experiment[27,28].

Group V (Acarbose + Calcipotriol/Betamethasone group n=6): Skin inflammation was induced as detailed in group II. Mice of this group received Glucobay treatment

and Calcipoheal-Cort ointment application as described in groups III and IV respectively.

IV- Experimental Procedure

Sacrifice of all the mice was done on the 7th day by cervical dislocation under 100 mg/kg pentobarbital sodium anesthesia administered intra¬peritoneally[29]. Back skin specimens were subjected to the following studies:

A. Light microscopic studies

Specimens were processed for paraffin sections (5 µm) which were subjected to the following stains:

1. Hematoxylin and Eosin (H&E)[30].
2. Immunohistochemical staining[31] for S100 protein. It was done according to the staining protocol provided by the UltraVision Detection System, a labeled streptavidin-biotin immune-enzymatic antigen detection kit, TP-015-HD, Thermo Fisher Scientific, Fremont, USA.

B. Electron microscopic study

Fine fragments of skin specimens were obtained. Prefixation was done in glutaraldehyde 2.5% followed by postfixation in osmium tetraoxide 1%. Dehydration was done in alcohol, clearing in propylene oxide and embedding in epoxy resin[32]. Ultrathin sections were stained with uranyl acetate-lead citrate[33]. Transmission electron microscope JEOL (JEM-1400 TEM) was used for examination of the sections. The images were captured by CCD camera, model AMT, at Electron Microscope Research Unit, Faculty of Agriculture, Cairo University.

C. Morphometric study

The following parameters were measured in randomly chosen, non-overlapping ten fields in each section:

1. Mean epidermal thickness in H&E stained sections [x200].
2. Mean number of S100 immuno-positive keratinocytes in S100 immuno-stained sections [x400].

Leica Qwin 500 LTD software image analysis computer system (Cambridge, England) was used for image analysis at the Histology department, Faculty of Medicine, Cairo University.

D. Statistical analysis

Statistical analysis of the morphometric measurements was done by "IBM SPSS statistics 23" and the data were reported as mean ± standard deviation (SD). To determine the statistical significance, One-way analysis of variance (ANOVA) followed by "Tuckey" post-hoc test were used. When "*P value*" was < 0.05, the differences were considered to be statistically significant[34].

RESULTS

A) General observations

No deaths were noticed in all mice during the experiment. Mice of both control subgroups showed the same macroscopic and microscopic picture. Group I mice showed apparently normal back skin all throughout the experiment (Figure 1a). IMQ treated mice (group II) showed psoriasis-like signs of inflammation in the form of redness (erythema) of the back skin and scaling. Erythema started at day 2, and increased in severity reaching a peak at day 7. Scaling started at day 3, but progressed rapidly at days 5, 6 and 7 (Figure 1b). Mice treated with acarbose (group III) and calcipotriol/betamethasone (group IV) showed less signs of inflammation with milder erythema and sparser scales, and the whole process was delayed 1 day as compared to group II (Figure 1c&d respectively). Combination of both treatments (group V) markedly attenuated of the inflammation as only slight erythema and was noticed starting day 4 and didn't increase in severity till day 7 (Figure 1e).

B) Light microscopic results

• H&E stained sections

Normal histological structure of the thin skin was illustrated by sections of group I. The epidermis comprised few layers of keratinocytes arranged as five strata; starting with the deepest, stratum basale, then, spinosum, granulosum, lucidum and the most superficial, stratum corneum. Dermal-epidermal junctions were flat except for involutions of the hair follicles. The dermis contained densely packed hair follicles, sebaceous glands and blood vessels (Figure 2a).

Group II sections demonstrated epidermal hyperplasia with strong epidermal thickening (acanthosis), marked thickening of stratum corneum (hyperkeratosis), in addition to presence of nuclei in some areas of stratum corneum (parakeratosis). Many keratinocytes showed vacuolated cytoplasm and pyknotic nuclei. Abundant elongated epidermal rete ridges were observed along with abundant infiltrates of mononuclear inflammatory cells in the dermis including lymphocytes, macrophages and mast cells (Figure 2b).

Examination of sections of treated groups (groups III and IV), illustrated that the changes observed in group II were ameliorated as they demonstrated less acanthosis and hyperkeratosis as well as fewer areas of parakeratosis. In addition, few keratinocytes showed vacuolated cytoplasm and pyknotic nuclei. Group III sections showed few elongated epidermal rete ridges while group IV sections showed almost flat dermal-epidermal junction except where hair follicles were present. In addition, sections of group IV showed many areas of inflammatory infiltrations (Figures 2c & 2d).

The changes caused by IMQ seen in group II were markedly diminished in sections of group V as they showed almost normal histological structure. Most of the keratinocytes showed normal morphology and unaffected nuclei. However, very few inflammatory infiltrates were still observed (Figure 2e).

• Immunohistochemical stained sections for S100 protien

Group I sections showed negative S100 immunoreaction in the epidermis and occasional S100 immuno-positive cells with cytoplasmic reaction around the hair follicles in the dermis (Figure 3a).

Sections of group II revealed numerous immuno-positive keratinocytes in the epidermis. The reaction appeared in the cytoplasm, nuclei and plasma membranes of the keratinocytes. Immuno-positive cytoplasmic reaction in multiple cells in the dermis was also noticed (Figure 3b).

Group III showed negative S100 immunoreaction in the epidermis, however, multiple immuno-positive cells were detected in the dermis very close to the basement membrane (Figure 3c). Group IV demonstrated multiple immuno-positive keratinocytes (Figure 3d). In both groups, few cells expressed immune-positive reactivity in the dermis around the hair follicles and in the endothelial lining of few blood vessels (Figures 3c and 3d). Negative S100 immunoreaction in the epidermis and few immuno-positive cells in the dermis of group V sections were noticed (Figure 3e).

C) Electron microscopic results

Ultrastructurally, sections from group I demonstrated the normal epidermal organization of keratinocytes as the five strata; stratum basale being the deepest layer, then, spinosum, granulosum, and finally stratum corneum, the most superficial one. The keratinocytes showed normal morphology of cytoplasm as well as normal euchromatic nuclei with prominent nucleoli. Desmosomal junctions connecting the keratinocytes together and hemidesmosomes connecting the epidermal-dermal interface were also observed (Figure 4).

Sections of group II revealed several histological changes in keratinocytes of all the layers. The markedly thickened stratum corneum demonstrated many wide spaces between the irregularly organized keratin scales. Marked reduction in cells of stratum granulosum was observed with disappearance of most of the granular keratinocytes. However, numerous electron dense keratohyaline granules were observed. The cytoplasm of many cells of stratum spinosum and stratum basale showed multiple vesicles while the nuclei of some cells showed heterochromatin condensed along their irregular and indented nuclear envelope and they were often shrunken. Wide intercellular spaces were detected between numerous stratum spinosum keratinocytes. Distinct areas of epidermal-dermal separation were also observed (Figures 5a-d).

Groups III and IV sections showed obvious improvement of the changes observed in group II, with less thickened stratum corneum and less numerous keratohyaline granules. Only few keratinocytes had heterochromatic, shrunken and indented nuclei and few small vesicles in the cytoplasm. Wide Intercellular spaces were noticed, however, intact epidermal-dermal interface was observed (Figures 6a and b and 7a and b).

Sections of group V demonstrated normal morphology of epidermis, with regularly organized keratin scales in stratum corneum with minimal spaces in between. Stratum granulosum showed few keratohyaline granules. The Keratinocytes had normal euchromatic nuclei with prominent nucleoli and normal cytoplasmic morphology, except for occasional cells that showed small vesicles in their cytoplasm and small intercellular spaces in between. Desmosomal junctions were seen connecting the keratinocytes together and hemidesmosomes connecting the epidermal-dermal interface were also noticed (Figures 8a-c).

D) Morphometric and statistical results (Table 1)

Morphometric and statistical results are illustrated in (Table 1).

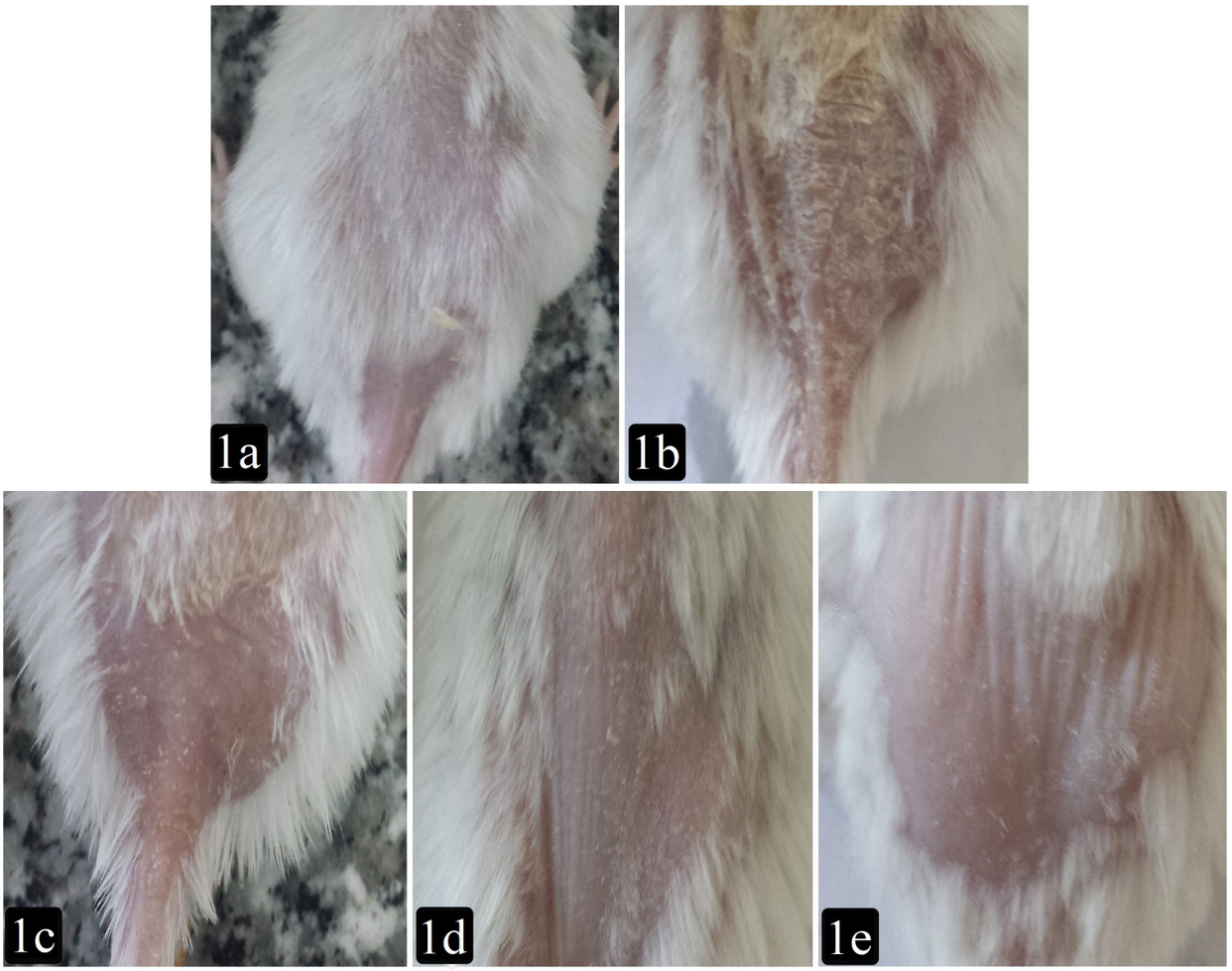

Fig. 1: Macroscopic picture of mice back skin at day 7.
a: Group I shows apparently normal back skin.
b: Group II shows psoriasis-like signs of skin inflammation in the form of erythema and scaling.
c: Group III and d: Group IV show mild erythema and sparse scales.
e: group V shows only slight erythema.

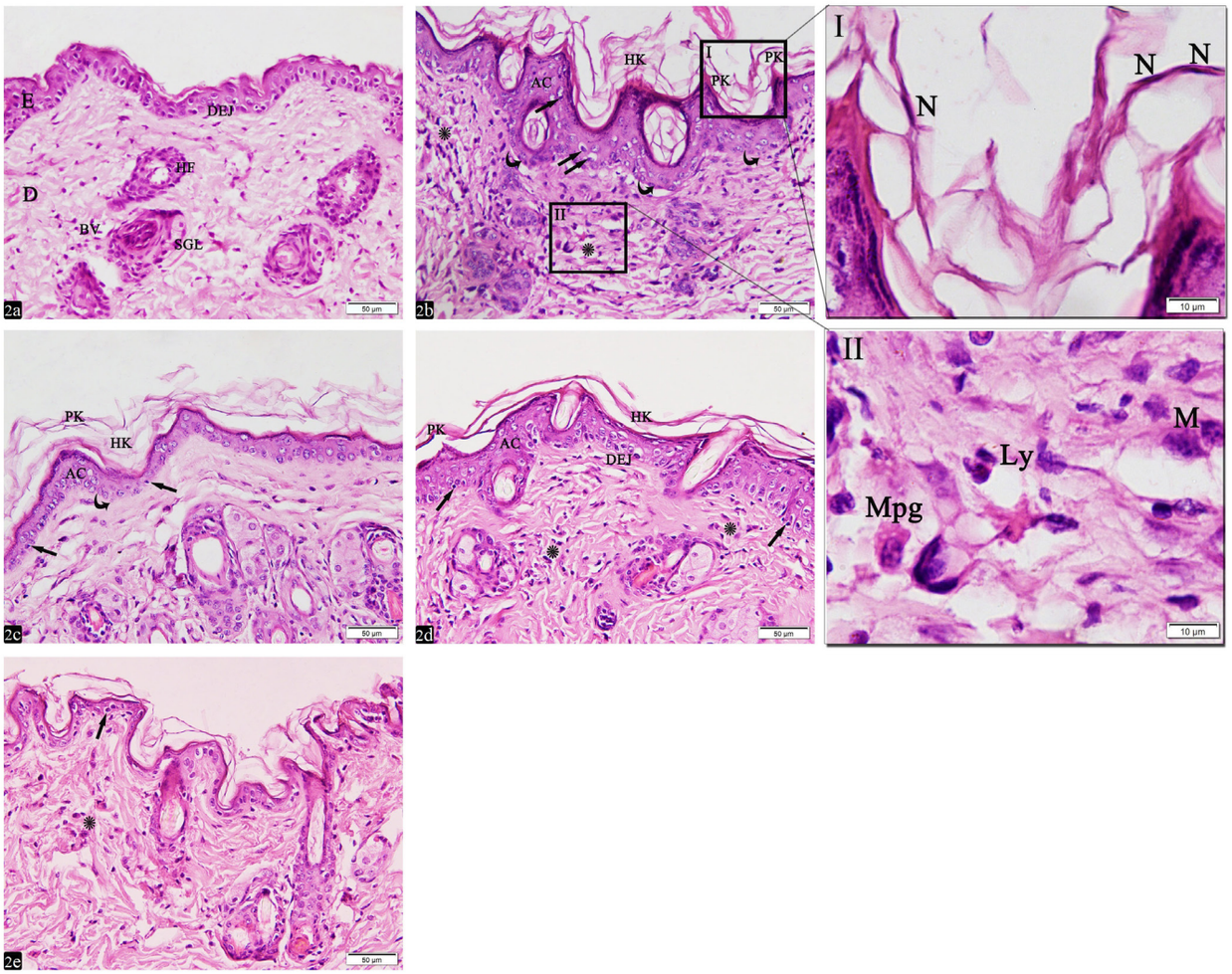

Fig. 2: Photomicrographs of H&E-stained skin sections.
a: Group I shows the epidermis (E), flat dermal-epidermal junction (DEJ) and dermis (D) containing hair follicles (HF), sebaceous glands (SGL) and blood vessels (BV) [x200].
b: Group II shows strong acanthosis (AC), marked hyperkeratosis (HK) and parakeratosis (PK). Many keratinocytes shows vacuolated cytoplasm and pyknotic nuclei (arrows). Elongated epidermal rete ridges (curved arrows) and abundant infiltrates of mononuclear inflammatory cells (asterisks) are noticed [x200]. Higher magnification of the boxed areas I and II shows retained nuclei of parakeratosis (N) in box I, and lymphocytes (Ly), macrophage (Mpg) and mast cells (M) of mononuclear inflammatory infiltration in box II [x1000].
c: Group III shows mild acanthosis (AC) and hyperkeratosis (HK) as well as few areas of parakeratosis (PK). Few keratinocytes showed vacuolated cytoplasm and pyknotic nuclei (arrows). An elongated epidermal rete ridge (curved arrow) is also observed [x200].
d: Group IV shows mild acanthosis (AC) and hyperkeratosis (HK), few areas of parakeratosis (PK) and few keratinocytes with vacuolated cytoplasm and pyknotic nuclei (arrows). Flat dermal-epidermal junction (DEJ) are noticed, in addition to many areas of inflammatory infiltrations (asterisks) [x200].
e: Group V shows almost normal histological structure except for occasional keratinocytes with vacuolated cytoplasm and pyknotic nuclei (arrows) and very few inflammatory infiltrates (asterisk) [x200].

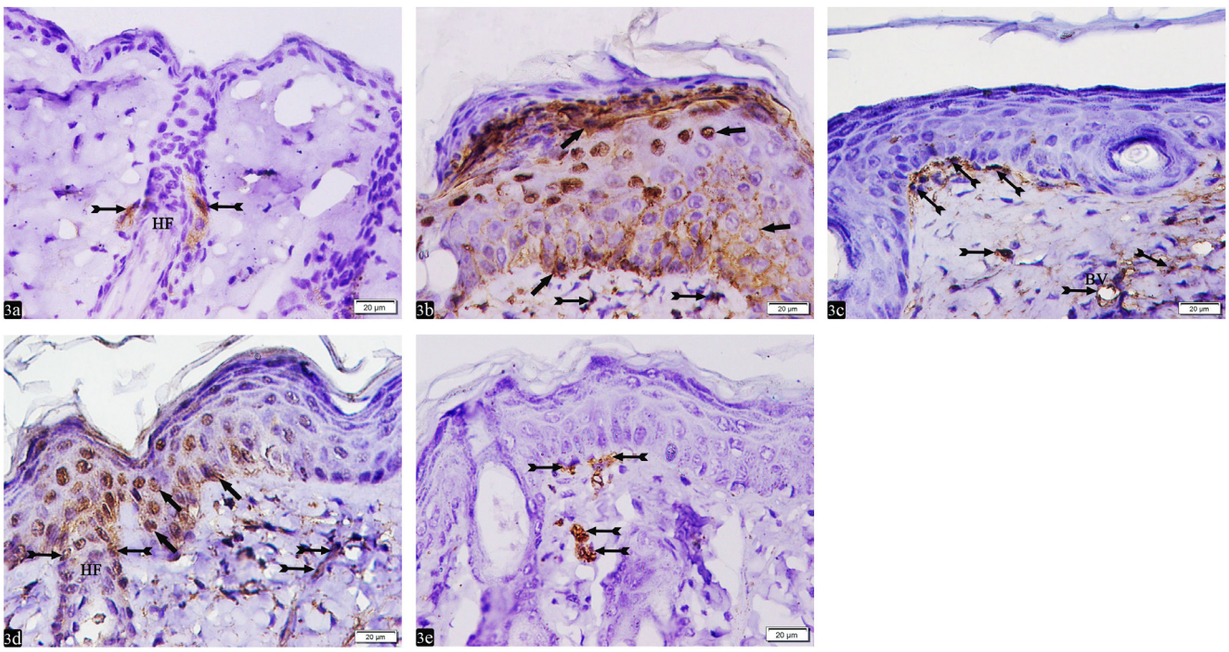

Fig. 3: Photomicrographs of S100 immuno-stained skin sections.
a: Group I shows negative S100 immunoreaction in the epidermis and occasional S100 immuno-positive cells in the dermis (bifid arrows) around the hair follicles (HF) [x400].
b: Group II shows numerous immuno-positive keratinocytes (arrows) and multiple immuno-positive cells in the dermis (bifid arrows) [x400].
c: Group III shows negative S100 immunoreaction in the epidermis and multiple cells in the dermis with immuno-positive reactivity (bifid arrows) and in the endothelium of few blood vessels (BV) [x400].
d: Group IV shows multiple keratinocytes with immuno-positive reactivity (arrows). Few immune-positive cells scattered in the dermis (bifid arrows) and around the hair follicles (HF) are seen [x400].
e: Group V shows negative S100 immunoreaction in the epidermis and few immuno-positive dermal cells (bifid arrows) [x400].

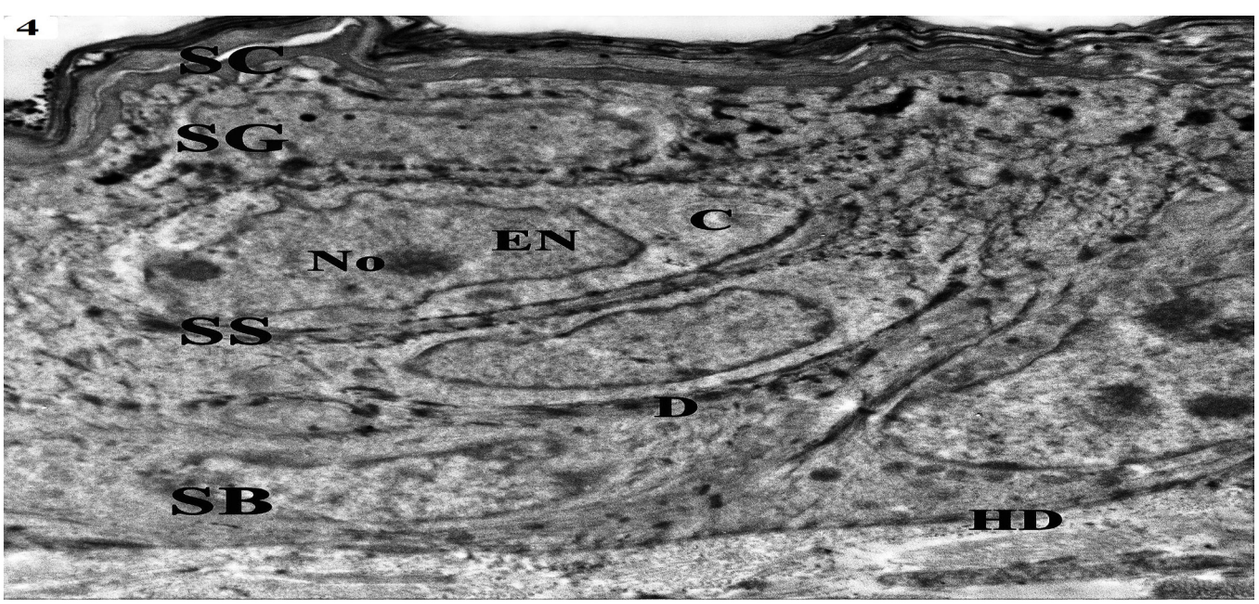

Fig. 4: Electron micrograph of a skin section from group I.
Shows keratinocytes organized as five strata; stratum basale (SB), spinosum (SS), granulosum (SG) and corneum (SC). Their cytoplasm (C) shows normal morphology as well as normal euchromatic nuclei (EN) with prominent nucleoli (No). Desmosomal (D) and hemidesmosomal (HD) junctions are observed [x5000].

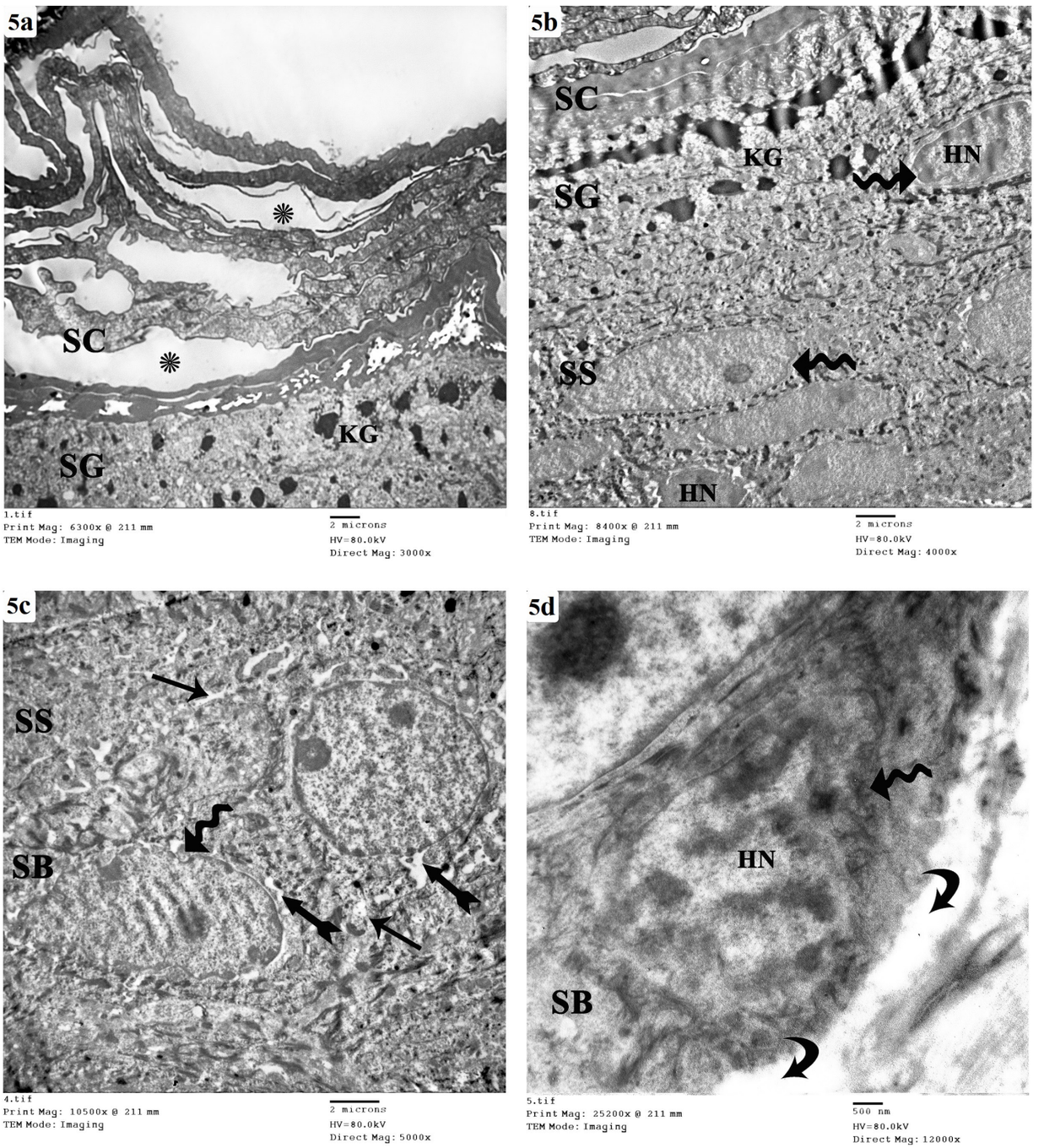

Fig. 5: Electron micrographs of skin sections from group II.
a: Shows many wide spaces (asterisks) between the irregularly organized keratin scales of markedly thickened stratum cornum (SC). Disappearance of most of granular keratinocytes is noted, however, numerous electron dense keratohyaline granules (KG) are observed in stratum granulosum (SG) [x3000].
b: Shows part of stratum corneum (SC), large amounts of electron dense keratohyaline granules (KG) with absence of granular keratinocytes in stratum granulosum (SG) and some cells of stratum spinosum (SS) with often shrunken heterochromatic nuclei (HN) with the chromatin condensed along their irregular and indented nuclear envelope (wavy arrows) [x4000].
c: Shows keratinocytes of stratum spinosum (SS) and stratum basale (SB) revealing multiple vesicles in their cytoplasm (bifid arrows), irregular and indented nuclear envelope (wavy arrows) and wide intercellular spaces (arrows) [x5000].
d: Shows a keratinocyte of stratum basale (SB) with a shrunken heterochromatic nucleus (HN) and irregular and indented nuclear envelope (wavy arrow). Distinct areas of epidermal-dermal separation are observed (curved arrows) [x12000].

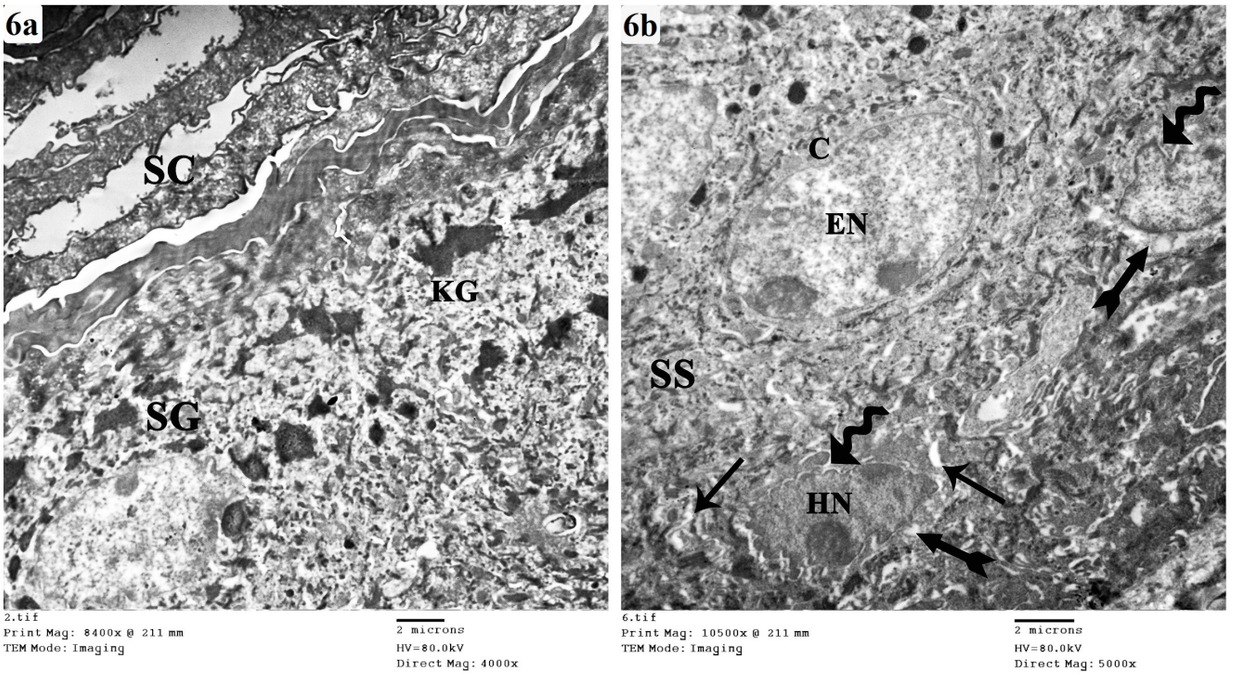

Fig. 6: Electron micrographs of skin sections from group III.
a: Shows thickened stratum corneum (SC) and many keratohyaline granules (KG) in stratum granulosum (SG) [x4000].
b: Shows keratinocytes of stratum spinosum (SS) with shrunken, heterochromatic (HN) and indented (wavy arrows) nuclei and few small vesicles in the cytoplasm (bifid arrows). Wide Intercellular spaces are seen (arrows), however, one keratinocyte with euchromatic nucleus (EN) and normal cytoplasmic (C) morphology is also noticed [x5000].

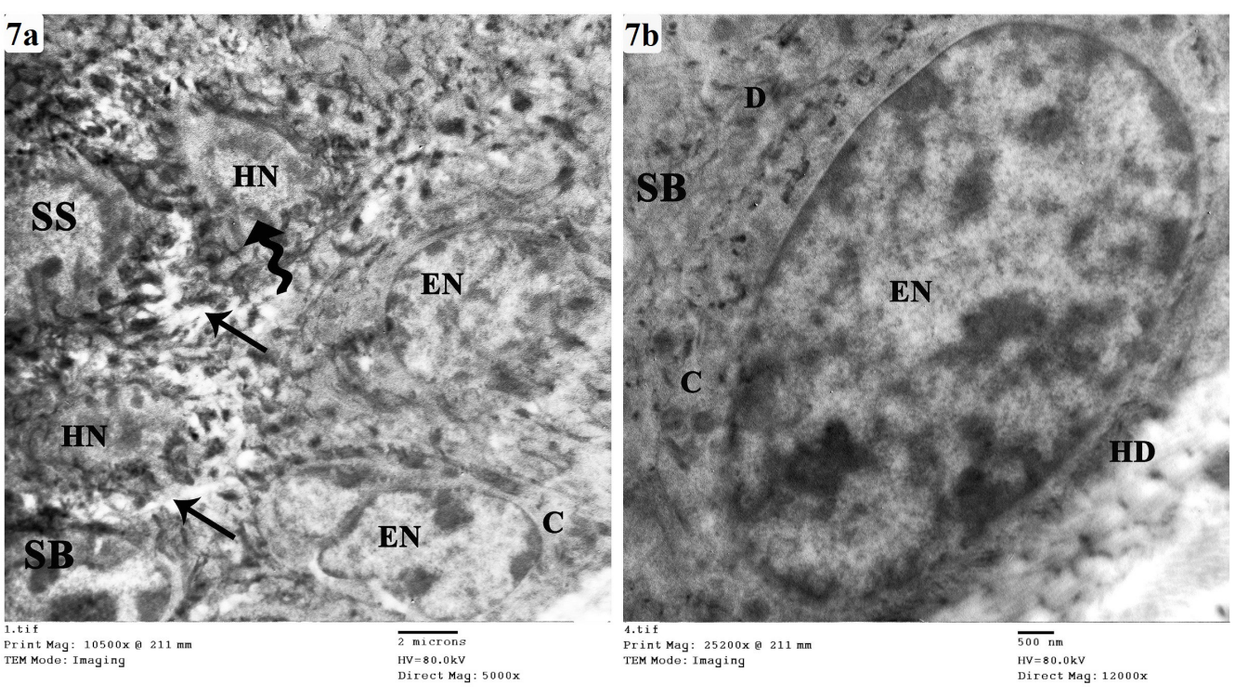

Fig. 7: Electron micrographs of skin sections from group IV.
a: Shows keratinocytes of stratum spinosum (SS) and stratum basale (SB). Two keratinocytes show shrunken heterochromatic (HN) and indented (wavy arrow) nuclei. Wide Intercellular spaces are observed (arrows). The remaining keratinocytes have euchromatic nuclei (EN) and normal cytoplasmic (C) morphology [x5000].
b: Shows a keratinocyte of stratum basale (SB) with normal morphology of cytoplasm (C) as well as normal euchromatic nucleus (EN). Desmosomal junctions (D) connecting the keratinocytes together and hemidesmosomes (HD) connecting the epidermal-dermal interface are also observed [x12000].

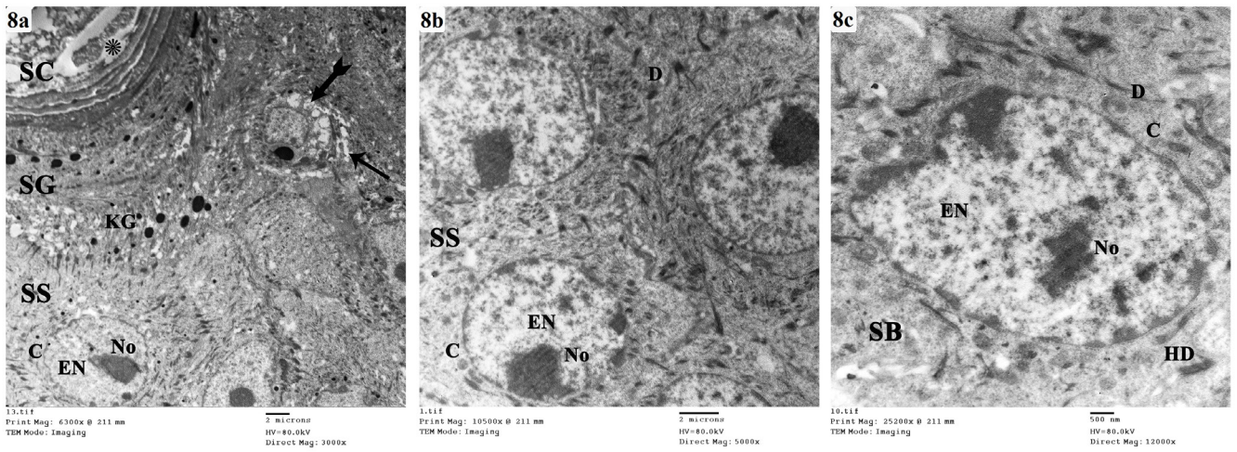

Fig. 8: Electron micrographs of skin sections from group V.
a: Shows regularly organized keratin scales in sratum corneum (SC) with minimal spaces in between (asterisks). Stratum granulosum (SG) show few keratohyaline granules (KG). The keratinocytes have normal euchromatic nuclei (EN) with prominent nucleoli (No) and normal cytoplasmic (C) morphology, except for occasional cells that show small vesicles in their cytoplasm (bifid arrows) and small intercellular spaces in between (arrows) [x3000].
b: Shows keratinocytes of stratum spinosum (SS) revealing normal euchromatic nuclei (EN) with prominent nucleoli (No) and normal cytoplasmic (C) morphology. Desmosomal junctions (D) are noticed connecting the keratinocytes together [x5000].
c: Shows a keratinocyte of stratum basale (SB) revealing normal euchromatic nucleus (EN) with prominent nucleolus (No) and normal cytoplasmic (C) morphology. Desmosomal junctions (D) are noticed connecting the keratinocytes together and hemidesmosomes (HD) connecting the epidermal-dermal interface are also observed [x12000].

Table 1: Mean values (±SD) of the epidermal thickness and S100 immuno-positive keratinocytes.

Group	Control	IMQ	Acarbose	Calcipotriol/ Betamethasone	Acarbose+Calcipotriol/Betamethasone
Epidermal thickness (µm)	22.77±1.63	92.41±10.05*	39.84±1.13○	37.32±1.50○	27.09±2.14□
S100 immuno-positive keratinocytes	-	19±1.41*	-	10.80±1.03○#	-

Statistical significance (p<0.05):

*Significant compared to control group.

○ Significant compared to control and IMQ groups.

□ Significant compared to IMQ, acarbose and calcipotriol/betamethasone groups.

Significant compared to acarbose and calcipotriol/betamethasone groups.

DISCUSSION

Psoriasis is considered to be one of the most researched skin diseases[4]. Although several psoriasis treatment modalities exist, management of psoriasis continues to be a challenging point in clinical medicine, and new treatment choices beyond the conventional ones are truly needed[35].

In the present study IMQ (Aldara cream) was used to induce psoriasis-like skin inflammation in BALB/c mice. The IMQ mouse model has become the most commonly used animal model of psoriasis since its first publication in 2009[26]. This model was chosen for its several advantages including fast response, relative inexpensiveness[36], convenience and simplicity[11]. Most importantly, the skin lesions caused by IMQ in mice remarkably mirror human psoriasis both phenotypically and histologically[37] as well as in regards to the genes implicated in epidermal development[22]. Most of the psoriasis mimicking studies using the IMQ mouse model are performed using BALB/c strain. Studies propose that IMQ responses could be strain-specific. For instance, following IMQ application, skin lesions in BALB/c develop more rapidly than other strains[11].

In the current work, group II mice developed psoriasis-like signs of inflammation following IMQ application, in the form of erythema and scaling of back skin that progressed throughout the duration of the experiment. These signs which phenocopy important features of human psoriasis have been previously reported by various studies that applied this model with the same IMQ dose on BALB/c mice for the same duration[24-26].

Microscopically, IMQ induced several histological changes in group II characterized by significantly marked acanthosis, with abundant elongated epidermal rete ridges and hyperkeratosis with some areas of parakeratosis. These changes are in agreement with the findings of prior IMQ model studies[7, 22, 24 and 38].

Skin turnover describes the transformation of basal keratinocytes into anucleate corneocytes, which in normal skin occurs over about 50 days, while in psoriatic skin, it only takes 5 days. This results from disturbance of the homeostasis of the epidermis which is normally maintained by a well-organized balance of differentiation and renewal processes[4]. Acanthosis has been attributed to an increase

in cell number as well as size. It was also described to display as elongated rete ridges with bulbous tips[39]. Rapid keratinocyte proliferation leading to acanthosis[40] has also been explained by continuous release of inflammatory factors from activated T lymphocytes leading to the presence of a sustained set of signals that results in epidermal hyperplasia[8]. Parakeratosis is an epidermal differentiation abnormality, a typical phenomenon for psoriasis skin lesions[26,41] and the underlying cause of scaling of the skin[26].

The presence of many keratinocytes with vacuolated cytoplasm and pyknotic nuclei demonstrated in group II has been previously reported following IMQ application[38]. It has been described that massive epidermal cell death is one of the early phenomena following the application of IMQ. In addition, necroptosis was hypothesized to have a major role in the death of keratinocytes. Furthermore, necroptotic keratinocytes have been considered the main triggers of inflammation by the production of damage-associated molecular patterns[7].

Abundant dermal infiltrates of mononuclear inflammatory cells including lymphocytes, macrophages and mast cells have been observed in group II. Psoriatic lesions exhibit dense infiltrates of inflammatory cells comprised of T lymphocytes, DCs[40,42], macrophages[42] and mast cells[43,44] in the dermis. IMQ activates pro-inflammatory signaling pathways through the ligation of TLR7/8 on DCs[36]. Mast cells, which are attracted to the lesion by the chemokines produced by keratinocytes, play an essential role in magnifying the inflammatory process[44]. Psoriasis-resembling skin inflammation triggered by IMQ is characterized by an imbalance in IL-23/IL-17 axis, with IL-23 and IL-17 are upregulated in patients suffering from psoriasis and psoriasis-like mice both[45]. It has been revealed that DCs release IL-23 to activate Th17 cells to produce large amounts of psoriatic cytokines, including IL-17 and IL-22[40]. These cytokines stimulate the hyper-proliferation of keratinocytes[40,46] as well as their production of further inflammatory factors such as antimicrobial peptides (AMPs)[47] which amplify the psoriatic inflammatory process[40].

Among the AMPs, S100 proteins have gained a notable interest as a principal factor in the pathogenesis of psoriasis. Psoriatic skin has displayed overexpression of S100A7, S100A8, and S100A9[4,21], S100A2 and S100A15[21]. Prominent co-expression of the homologue S100 proteins S100A7, S100A8, S100A9 and S100A12, has been demonstrated suggesting their co-regulation and synergy[48].

In psoriatic skin, S100A7 overexpression in keratinocytes is located in the nucleus and the cytoplasm[48]. S100A15 is produced by basal keratinocytes, DCs and the endothelium of blood vessels. Moreover, in mice, S100A7 shares an ancestral protein with S100A15[19]. S100A8 and S100A9 together form a complex[49] produced by DCs, macrophages, keratinocytes and endothelial cells. It has been reported that S100A8/S100A9 complex is immensely produced by psoriatic keratinocytes[19,50]. It was demonstrated that both S100A8 and S100A9 localize in the peripheral cytoplasm, besides, S100A9 is also detected within the plasma membrane as well. They are both expressed in stratum granulosum, spinosum and basale[51]. As for S100A12, it is detected in the suprabasal layers of the epidermis[21].

The previous data support our S100 immunohistochemical findings which revealed significantly numerous S100-positive keratinocytes in group II, with the reaction seen in the cytoplasm, nuclei and plasma membranes of keratinocytes. In addition, immuno-positive reaction was seen in multiple cells in the dermis. While Group I sections showed negative S100 immunoreaction in the epidermis and occasional S100 immuno-positive cells around the hair follicles in the dermis. In agreement with our results are the findings of prior studies that applied the IMQ model and displayed an increase in the expression of the inflammatory protein S100A8 in the epidermis. Also, it has been reported that necroptotic keratinocytes produce damage-associated molecular patterns, as S100 proteins[7]. Furthermore, it was demonstrated that mRNA levels of S100A8, and S100A9, were markedly increased in IMQ-treated mice[28].

Ultrastructurally, group II in our study demonstrated a significantly thickened stratum corneum with many wide spaces between irregularly organized keratin scales and numerous electron dense keratohyaline granules. Similar results were previously obtained by previous studies[38]. Moreover, our sections displayed a marked reduction in cells of stratum granulosum with disappearance of most of the granular keratinocytes. This is in accordance with prior IMQ model studies[26] as well as studies done on samples obtained from psoriatic plaques of psoriasis patients[35,39]. This finding, described as “hypogranulosis” was credited to the aberrant differentiation of keratinocytes[40].

As for stratum spinosum and stratum basale of group II, many keratinocytes showed multiple cytoplasmic vesicles. The same finding was similarly demonstrated in prior studies[38,52]. In addition, the nuclei of some cells showed heterochromatin condensed along their irregular and indented nuclear envelope and they were often shrunken. This could be explained by the effect of IMQ application, which has been described to massively disturb the epidermal integrity and lead to keratinocyte apoptosis[41]. Wide intercellular spaces were detected between numerous stratum spinosum keratinocytes, a feature previously reported by IMQ induced psoriasis-like studies[38] and prior electron microscopic studies on human psoriasis[52] that explained it by reduction of desmosomes, indicating alteration of cell-cell adhesion. Finally, distinct areas of epidermal-dermal separation were observed. It was previously suggested that in psoriasis, lymphocytes and neutrophils release proteolytic enzymes that affect laminin and collagen type IV, the most important macromolecules in the epidermal basement membrane, resulting in loss of its integrity[39].

Regarding groups III and IV of the current work, we treated IMQ induced psoriasis mice with acarbose and calcipotriol/betamethasone respectively. Acarbose, is considered one of the safest available antidiabetic drugs[53] that has also been reported to lower some inflammatory markers in diabetic patients as well as in arthritic mice[54]. The combination of vitamin D3 analogue "calcipotriol" and the corticosteroid "betamethasone" is broadly prescribed for treatment of psoriasis[47,55 and 56]. Vitamin D3 analogues stimulate keratinocyte differentiation, inhibit keratinocyte proliferation and inhibit T cells, DCs and keratinocytes cytokine production. As for corticosteroids, they have powerful anti-inflammatory effects with wide-ranging immunosuppressive functions through blocking inflammatory pathways and triggering apoptosis[47,56].

The treated groups in our study, groups III and IV, showed less signs of inflammation with milder erythema and sparser scales as compared to group II. Upon microscopical examination, the changes observed in group II were ameliorated in both groups revealing histological findings almost comparable to each other. They demonstrated significantly less acanthosis compared to group II, however still significantly increased in comparison to the control group. This is accordance with a previous study[24] that investigated the effects of acarbose on IMQ-induced psoriasis-like inflammation of skin of BALB/c mice which exhibited reduced erythema and scaling over the whole period of treatment as well as significant decrease of the epidermal thickness. Also, in agreement with our observations, calcipotriol[8] and betamethasone[28] have been reported to significantly reduce erythema and scaling in IMQ treated mice. Moreover, calcipotriol/betamethasone therapy has been stated to hinder the epidermal thickening in skin biopsy samples of psoriasis patient[56,57].

Prior to our study it was previously demonstrated that acarbose decreased the inflammatory cellular infiltration in IMQ model of psoriasis. Moreover, it also decreased mRNA level of the pro-inflammatory IL-17 and IL-22 cytokines in the skin lesion[24]. They suggested that oral intake of acarbose influences the adaptive immune response indirectly through modulating the activation of DCs in the intestine. They also found that, similar to our results, acarbose alone wasn't able to fully suppress the psoriatic changes. Thus, they recommended the combination of acarbose with other treatments of psoriasis, which we applied in group V. Going with our results, it has been formerly demonstrated that topical application of calcipotriol suppressed the inflammatory cellular infiltration in skin of mice with IMQ induced dermatitis[58]. In addition, calcipotriol/betamethasone therapy has been stated to suppress T cells infiltration in skin specimens obtained from psoriatic patients[56,57]. Moreover, calcipotriol[58] and betamethasone were reported to inhibit the increase in the mRNA levels of IL-17 and IL-22 in psoriasis induced by IMQ in mice. However, betamethasone a had minor effect on IL-23 level, indicating that it exerted its anti-inflammatory effects by suppressing Th1 cells, Th17 cells as well as keratinocytes, but it couldn't be able to directly affect DCs rendering them triggered by IMQ[28]. This could explain the presence of many inflammatory infiltration areas in our group IV.

As for the S100 immunohistochemical staining of group III, it showed negative immunoreactivity in the epidermis, while in group IV sections, the immuno-positive keratinocytes significantly decreased as compared to group II, strengthening the amelioration signs observed both morphologically and microscopically, attributed to acarbose and calcipotriol/betamethasone anti-inflammatory functions. A significant increase in group IV was noted as compared to control and group III, supporting our finding of many inflammatory infiltration areas in group IV. It is worth mentioning that betamethasone has been formerly reported to decrease the mRNA levels of S100A8 and S100A9 significantly in IMQ-induced skin lesions in mice[28]. Furthermore, Vitamin D3 analogues were described to be effective in psoriasis treatment through modulating the expression of S100A7/ S100 A15[19,46 and 58].

Ultrastructure examination of sections of groups III and IV mirrored the obvious improvement of the changes observed in group II, as it showed less thickened stratum corneum, less numerous keratohyaline granules and fewer affected karatinocytes. Similar findings featuring an overall improvement of the psoriatic changes were reported by a previous ultrastructural study on psoriatic skin biopsies of patients treated with calcipotriol ointment, confirming its efficacy in normalizing the process of keratinization[59].

In group V, we combined both treatments, acarbose and calcipotriol/betamethasone. This combination markedly suppressed the inflammation as only slight erythema was noticed. Microscopic examination showed that changes caused by IMQ seen in group II were evidently diminished as they showed almost normal histological structure. The epidermal thickness decreased significantly as compared to groups II, III and IV, besides, it showed a non-significant increase compared to the control. Most of the keratinocytes showed normal morphology and unaffected nuclei. Nevertheless, very few inflammatory infiltrates were still observed. Negative epidermal immune-reactivity was noticed in S100 stained sections. Parallel findings were seen ultrastructurally, comprising normal morphology of epidermis, with regularly organized keratin scales in stratum corneum, few keratohyaline granules, normal keratinocytes morphology except for occasional cells and intact epidermal-dermal interface.

CONCLUSION

The present work demonstrated that acarbose treatment had the ability to attenuate psoriasis-like skin inflammation induced by IMQ in mice to an extent comparable to calcipotriol/betamethasone. The combination of both treatments exerted a more marked beneficial effect, which holds a great promise for combining acarbose with other psoriasis treatment modalities.

CONFLICTS OF INTEREST

There are no conflicts of interest.

REFERENCES

1. World Health Organization: Global report on psoriasis in World Health Organization (2016) ISBN 978 92 4 156518 9.
2. El Malki K, Karbach SH, Huppert J, Zayoud M, Reissig S, Schüler R, Nikolaev A, Karram K, Münzel T, Kuhlmann CR, Luhmann HJ, von Stebut E, Wörtge S, Kurschus FC and Waisman A: An alternative pathway of imiquimod-induced psoriasis-like skin inflammation in the absence of interleukin-17 receptor a signaling in J. Invest. Dermatol. (2013) 133(2): 441-51.
3. Varma SR, Sivaprakasam TO, Mishra A, Prabhu S, M R and P R: Imiquimod-induced psoriasis-like inflammation in differentiated Human keratinocytes: Its evaluation using curcumin in Eur. J. Pharmacol. (2017) 813: 33-41.
4. Benhadou F. Mintoff D and del Marmol V: Psoriasis: Keratinocytes or Immune Cells – Which Is the Trigger? in Dermatology (2019) 235: 91-100.
5. Singh S, Young P and Armstrong AW: An update on psoriasis and metabolic syndrome: A meta-analysis of observational studies in PLoS ONE (2017) 12(7): e0181039.
6. Boehncke WH and Schoen MP: Psoriasis in Lancet 386 (2015) (9997): 983–994.
7. Alrefai H, Muhammad K, Rudolf R, Pham DA, Klein-Hessling S, Patra AK, Avots A, Bukur V, Sahin U, Tenzer S, Goebeler M, Kerstan A and Serfling E: NFATc1 supports imiquimod-induced skin inflammation by suppressing IL-10 synthesis in B cells in Nat. Commun. (2016) 25(7): 11724.
8. Lin Z, Ma M, Li H, Qi Q, Liu YT, Yan YX, Shen YF, Yang XQ, Zhu FH, He SJ, Tang W and Zuo JP: Topical administration of reversible SAHH inhibitor ameliorates imiquimod-induced psoriasis-like skin lesions in mice via suppression of TNF-α/IFN-γ-induced inflammatory response in keratinocytes and T cell-derived IL-17 in Pharmacol. Res. (2018) 129: 443-452.
9. Luo DQ, Wu HH, Zhao YK, Liu JH and Wang F: Original Research: Different imiquimod creams resulting in differential effects for imiquimod-induced psoriatic mouse models in Exp. Biol. Med. (Maywood) (2016) 241(16): 1733-1738.
10. OuYang Q, Pan Y, Luo H, Xuan C, Liu J and Liu J: MAD ointment ameliorates Imiquimod-induced psoriasiform dermatitis by inhibiting the IL-23/IL-17 axis in mice in Int. Immunopharmacol. (2016) 39: 369-376.
11. Swindell WR, Michaels KA, Sutter AJ, Diaconu D, Fritz Y, Xing X, Sarkar MK, Liang Y, Tsoi A, Gudjonsson JE and Ward NL: Imiquimod has strain-dependent effects in mice and does not uniquely model human psoriasis in Genome. Med. (2017) 9(1): 24.
12. Meng Y, Wang M, Xie X, Di T, Zhao J, Lin Y, Xu X, Li N, Zhai Y, Wang Y and Li P1: Paeonol ameliorates imiquimod-induced psoriasis-like skin lesions in BALB/c mice by inhibiting the maturation and activation of dendritic cells in Int. J. Mol. Med. (2017) 39(5): 1101-1110.
13. Ueyama A, Yamamoto M, Tsujii K, Furue Y, Imura C, Shichijo M and Yasui K: Mechanism of pathogenesis of imiquimod-induced skin inflammation in the mouse: a role for interferon-alpha in dendritic cell activation by imiquimod in J. Dermatol. (2014) 41(2): 135-43.
14. Owczarczyk-Saczonek A, Krajewska-Włodarczyk M, Kruszewska A, Placek W, Maksymowicz W and Wojtkiewicz J: Stem Cells as Potential Candidates for Psoriasis Cell-Replacement Therapy in Int. J. Mol. Sci.(2017) 18(10): E2182.
15. Hiebert P and Werner S: Targeting metabolism to treat psoriasis in Nat. Med. (2018) 24(5): 537-539.
16. Rosak C and Mertes G: Critical evaluation of the role of acarbose in the treatment of diabetes: patient considerations in Diabetes Metab. Syndr. Obes. (2012)5: 357–367.
17. Su B, Liu H, Li J, Sunli Y, Liu B, Liu D, Zhang P and Meng X: Acarbose treatment affects the serum levels of inflammatory cytokines and the gut content of bifidobacteria in Chinese patients with type 2 diabetes mellitus in J. Diabetes (2015) 7(5):729-39.
18. Golia E, Limongelli G, Natale F, Fimiani F, Maddaloni V, Pariggiano I, Bianchi R, Crisci M, D'Acierno L, Giordano R, Di Palma G, Conte M, Golino P, Russo MG, Calabrò R and Calabrò P: Inflammation and cardiovascular disease: from pathogenesis to therapeutic target in Curr. Atheroscler. Rep. (2014) 16(9): 435.
19. Batycka-Baran A, Maj J, Wolf R and Szepietowski JC: The new insight into the role of antimicrobial proteins-alarmins in the immunopathogenesis of psoriasis in J. Immunol. Res. (2014) 2014: 628289.
20. Wohn C: Mechanisms Of Psoriatic Plaque Formation In Mice. Off-set, Amsterdam, The Netherlands. Erlangen, Germany. (2015) pp: 11.
21. Eckert RL, Broome AM, Ruse M, Robinson N, Ryan D and Lee K: S100 proteins in the epidermis in J. Invest. Dermatol. (2004) 123(1): 23-33.
22. Bürger C, Shirsath N, Lang V, Diehl S, Kaufmann R, Weigert A, Han YY, Ringel C and Wolf P: Blocking mTOR Signalling with Rapamycin Ameliorates Imiquimod-induced Psoriasis in Mice in Acta. Derm. Venereol. (2017) 97(9): 1087-1094.

23. Huang SW, Chen YJ, Wang ST, Ho LW, Kao JK, Narita M, Takahashi M, Wu CY, Cheng HY and Shieh JJ: Azithromycin impairs TLR7 signaling in dendritic cells and improves the severity of imiquimod-induced psoriasis-like skin inflammation in mice in J. Dermatol. Sci. (2016) 84(1): 59-70.
24. Chen HH, Chao YH, Chen DY, Yang DH, Chung TW, Li YR and Lin C: Oral administration of acarbose ameliorates imiquimod-induced psoriasis-like dermatitis in a mouse model in Int. Immunopharmacol. (2016) 33: 70-82.
25. Chen W, Gong Y, Zhang X, Tong Y, Wang X, Fei C, Xu H, Yu Q, Wang Y and Shi Y: Decreased expression of IL-27 in moderate-to-severe psoriasis and its anti-inflammation role in imiquimod-induced psoriasis-like mouse model in J. Dermatol. Sci. (2017) 85(2): 115-123.
26. van der Fits L, Mourits S, Voerman JS, Kant M, Boon L, Laman JD, Cornelissen F, Mus AM, Florencia E, Prens EP and Lubberts E: Imiquimod-induced psoriasis-like skin inflammation in mice is mediated via the IL-23/IL-17 axis in J. Immunol. (2009) 182(9): 5836-45.
27. Liu X, Liu Y, Xu M, Li J, Teng X, Cheng H and Xia Y: Zinc finger protein A20 is involved in the antipsoriatic effect of calcipotriol in Br. J. Dermatol. (2016) 175(2): 314-24.
28. Mori H, Arita K, Yamaguchi T, Hirai M and Kurebayashi Y: Effects of Topical Application of Betamethasone on Imiquimod-induced Psoriasis-like Skin Inflammation in Mice in Kobe. J. Med. Sci. (2016) 62(4): E79-E88.
29. Bai S, Zhang Z, Hou S and Liu X: Influence of Different Types of Contact Hypersensitivity on Imiquimod-induced Psoriasis-like Inflammation in Mice in Mol. Med. Rep. (2016) 14(1): 671-680.
30. Kiernan J. Histological and histochemical methods: theory and practice. 3rd ed. Arnold publisher. London, New York & New Delhi. (2001) pp: 111-162.
31. Bancroft J and Gamble M. Theory and Practice of Histological Techniques. Staining methods. 7th ed., Churchill Livingstone Edinburgh. London, Madrid, Melbourne, New York and Tokyo. (2008) pp: 263-325.
32. Hayat MA. Chemical fixation. In: Principles and techniques of electron microscopy: biological applications. 4th ed., Cambridge University Press, Edinburg. UK. (2000) pp: 4-85.
33. Dykstra MJ and Reuss LE. Staining methods for semithins and ultra thins. In: Biological electron microscopy, theory, techniques and troubleshooting. 2nd ed. Kluwer Academic Publishers/Plenum Publishers. (2003) pp: 175-196.
34. Emsley R, Dunn G and White IR. Mediation and moderation of treatment effects in randomized controlled trials of complex interventions in Stat. Methods. Med Res. (2010) 19: 237-270.
35. Natsumi A, Sugawara K, Yasumizu M, Mizukami Y, Sano S, Morita A, Paus R and Tsuruta D: Re-investigating the Basement Membrane Zone of Psoriatic Epidermal Lesions: Is Laminin-511 a New Player in Psoriasis Pathogenesis? in J. Histochem. Cytochem. (2018) 66(12): 847-862.
36. Horváth S, Komlódi R, Perkecz A, Pintér E, Gyulai R & Kemény A: Methodological refinement of Aldara-induced psoriasiform dermatitis model in mice in Scientific Reports (2019) 9: 3685.
37. Kim CH, Yoo JK, Jeon SH, Lim CY, Lee JH, Koo DB and Park MY: Anti-psoriatic effect of myeloid-derived suppressor cells on imiquimod-induced skin inflammation in mice in Scand. J. Immunol. (2019) 89(3): e12742.
38. Okasha EF, Bayomy NA and Abdelaziz EZ: Effect of Topical Application of Black Seed Oil on Imiquimod-Induced Psoriasis-like Lesions in the Thin Skin of Adult Male Albino Rats in Anat. Rec. (Hoboken). (2018) 301(1): 166-174.
39. Eşrefoğlu M, Seyhan M, Aktaş A, Gül M and Öztürk F: Histopathological Findings and the Distribution of Laminin and Fibronectin in Psoriatic Skin in İnönü. Üniversitesi. Tıp. Fakültesi. Dergisi. (2005) 12(4): 217-222.
40. Nakajima K and Sano S: Mouse models of psoriasis and their relevance in J. Dermatol. (2018) 45(3): 252-263.
41. Walter A, Schäfer M, Cecconi V, Matter C, Urosevic-Maiwald M, Belloni B, Schönewolf N, Dummer R, Bloch W, Werner S, Beer HD, Knuth and van den Broek M: Aldara activates TLR7-independent immune defence in Nat. Commun. (2013) 4: 1560.
42. Kim TG, Kim DS, Kim HP and Lee MG: The pathophysiological role of dendritic cell subsets in psoriasis in BMB Rep. (2014) 47(2): 60-8.
43. Amberg N, Holcmann M, Stulnig G and Sibilia M: Effects of Imiquimod on Hair Follicle Stem Cells and Hair Cycle Progression in J. Invest. Dermatol. (2016) 136(11): 2140-2149.
44. Abdelnoor A and Al-Akl N: Factors Involved in the Pathogenesis of Psoriasis in Advanced Studies in Medical Sciences. (2013) 1(2): 75 – 94.
45. Chen Y, Zhang Q, Liu H, Lu C, Liang CL, Qiu F, Han L and Dai Z: Esculetin Ameliorates Psoriasis-Like Skin Disease in Mice by Inducing CD4+Foxp3+ Regulatory T Cells in Front. Immunol. (2018) 12(9): 2092.

46. Suzuki T, Tatsuno K, Ito T, Sakabe JI, Funakoshi A and Tokura Y: Distinctive downmodulation of plasmacytoid dendritic cell functions by vitamin D3 analogue calcipotriol in J. Dermatol. Sci. (2016) 84(1): 71-79.

47. Lovato P, Norsgaard H, Tokura Y and Røpke MA: Calcipotriol and betamethasone dipropionate exert additive inhibitory effects on the cytokine expression of inflammatory dendritic cell-Th17 cell axis in psoriasis in J. Dermatol. Sci. (2016) 81(3): 153-64.

48. Ekman AK, Vegfors J, Eding CB and Enerbäck C: Overexpression of Psoriasin (S100A7) Contributes to Dysregulated Differentiation in Psoriasis in Acta. Derm. Venereol. (2017) 97(4): 441-448.

49. Schonthaler HB, Guinea-Viniegra J, Wculek SK, Ruppen, Ximénez-Embún P, Guío-Carrión A, Navarro R, Hogg N, Ashman K and Wagner EF: S100A8-S100A9 protein complex mediates psoriasis by regulating the expression of complement factor C3 in Immunity. (2013) 39(6): 1171-81.

50. Xia C, Braunstein Z, Toomey AC, Zhong J and Rao X: S100 Proteins as an Important Regulator of Macrophage Inflammation in Front. Immunol. (2018) 8:1908.

51. Broome AM, Ryan D and Eckert RL: S100 protein subcellular localization during epidermal differentiation and psoriasis in J. Histochem. Cytochem. (2003) 51(5): 675-85.

52. Fleischmajer R, Kuroda K, Hazan R, Gordon RE, Lebwohl MG, Sapadin AN, Unda F, Iehara N and Yamada Y: Basement membrane alterations in psoriasis are accompanied by epidermal overexpression of MMP-2 and its inhibitor TIMP-2 in J. Invest. Dermatol. (2000) 115(5): 771-7.

53. Han X, Deng Y, Yu J, Sun Y, Ren G, Cai J, Zhu J and Jiang G: Acarbose Accelerates Wound Healing via Akt/eNOS Signaling in db/db Mice in Oxid. Med. Cell. Longev. (2017) 2017:7809581.

54. Chen HH, Chen DY, Chao YH, Chen YM, Wu CL, Lai KL, Lin CH, Lin CC: Acarbose Decreases the Rheumatoid Arthritis Risk of Diabetic Patients and Attenuates the Incidence and Severity of Collagen-induced Arthritis in Mice in Sci Rep. (2015) 18(5): 18288.

55. Kaur A, Katiyar SS, Kushwah V and Jain S: Nanoemulsion loaded gel for topical co-delivery of clobitasol propionate and calcipotriol in psoriasis in Nanomedicine. (2017) 13(4): 1473-1482.

56. Satake K, Amano T and Okamoto T: Low systemic exposure and calcemic effect of calcipotriol/betamethasone ointment in rats with imiquimod-induced psoriasis-like dermatitis in Eur. J. Pharmacol. (2018) 826: 31-38.

57. Fujiyama T, Ito T, Umayahara T, Ikeya S, Tatsuno K, Funakoshi A, Hashizume H and Tokura Y: Topical application of a vitamin D3 analogue and corticosteroid to psoriasis plaques decreases skin infiltration of TH17 cells and their ex vivo expansion in J. Allergy. Clin. Immunol. (2016) 138(2): 517-528.e5.

58. Kusuba N, Kitoh A, Dainichi T, Honda T, Otsuka A, Egawa G, Nakajima S, Miyachi Y and Kabashima K: Inhibition of IL-17-committed T cells in a murine psoriasis model by a vitamin D analogue in J. Allergy. Clin. Immunol. (2018) 141(3): 972-981.e10.

59. Cavicchini S, Brezzi A, Gasparini G and Caputo R: Skin ultrastructure after calcipotriol treatment: a transmission electron microscopic and freeze-fracture study on psoriatic patients in Acta. Derm. Venereol. (1996) 76(3): 186-9.

الملخص العربى

دراسة هستولوجيه مقارنة على الدور الوقائي للأكاربوز والكالسيبوتريول/بيتاميثازون في نموذج الفأر المصاب بالتهاب الجلد المشابه للصدفية الناجم عن الإيميكيمود

سارة محمد الغندور، مروة محمد صبري، منال علي عبد المحسن

قسم علم الأنسجة، كلية الطب، جامعة القاهرة، القاهرة، مصر

مقدمة: تعتبر الصدفية مرض جلدي مناعي ذاتي من علاماته ظهور طفح جلدى وتقشر. يتم استخدام الايميكيمود مؤخرا لحث التهاب الجلد في الفئران لانتاج نموذج للصدفيه.

الهدف من العمل: تقييم الامكانيه الوقائية المحتمله للأكاربوز على التهاب الجلد المشابه للصدفيه الناجم عن الإيميكيمود فى ذكور الفئران البالغة ، ومقارنته بالكالسيبوتريول/بيتاميثازون المطبق على نفس نموذج الفأر المصاب الصدفية.

المواد والطرق: تم تصنيف أربعة وثلاثين فأرا BALB / c كالمجموعات التالية: ١(الضابطة)، ٢(الإيميكيمود): نموذج الايميكيمود عن طريق كريم الدارا المستخدم موضعيا، ٣(الأكاربوز) نموذج الإيميكيمود المعالج بـجلوكوباى عن طريق الفم ، ٤(الكالسيبوتريول/بيتاميثازون) نموذج الإيميكيمود المعالج بمرهم الكالسيبوهيل-كورت و٥(الكالسيبوتريول/ بيتاميثازون+الأكاربوز) نموذج الإيميكيمود المعالج بمرهم الكالسيبوتريول/بيتاميثازون والأكاربوزمعا. تم صباغة مقاطع الجلد بصبغة الهيماتوكسلين والإيوسين والصبغة الهستوكيميائية المناعية S100الي جانب عمل دراسة مجهرية إلكترونية. تم قياس متوسط سماكة البشرة ومتوسط عدد الخلايا التقرنية الموجبة مناعيا لل S100 وتم تحليل القياسات إحصائيا.

النتائج: أظهرت المجموعة الثانية علامات لالتهاب الجلد تشبه الصدفية . أظهرت فئران المجموعة الثالثة والرابعة علامات أقل شدة للالتهابات والتي تم تحسنها بشكل ملحوظ عن طريق الجمع بين العلاجين. أظهرت المجموعة الثانية زيادة ذات دلالة إحصائية فى كثافة طبقة الجلد، ووفرة من الارتشاح الخلوي الالتهابي في الأدمة. أظهرت المجموعتان الثالثة والرابعة تحسنا ملحوظا في هذه التغييرات التي تضاءلت بشكل ملحوظ في المجموعة الخامسة حيث انها أظهرت بنية نسيجية طبيعية تقريبا.

الإستنتاج: كان للأكاربوز تأثيرا نافعا بشكل عام على نموذ الفأر المحاكي للصدفيه المستحث بواسطة الإيميكيمود ، والذي يشبه تقريباً ذلك الذي أظهره كالسيبوتريول/بيتاميثازون. ومع ذلك، فإن الجمع بين كل من العلاجين أظهر تأثيرا علاجيا أكثر قوة.